ARTICLE
Reproducible Quantitative Stimulation Allows New Analysis of Crayfish Muscle Receptor Organ Responses

Anthony E. Ambrosini & Alan Gelperin
Princeton Neuroscience Institute, Princeton University, Princeton, NJ 08544.

The crustacean muscle receptor organ (MRO) has provided a particularly accessible preparation for the study of sensory coding, which has been widely used in introductory laboratory courses incorporating extracellular recording from sensory nerves in living preparations. We describe three innovations to the standard laboratory exercise using the MRO: (1) a new form of suction electrode to facilitate extracellular recording; (2) a new, Arduino-driven actuator to allow reproducible and quantifiable mechanical stimulation of the MRO; and (3) a new approach to the crayfish abdomen preparation that allows linear extension of the MRO muscles. These novel approaches allow the collection of data sets comprised of sensory cell spike trains under software control as important mechanical stimulus parameters are varied systematically through software. This additional level of user control facilitates a more robust quantitative approach to the analysis of MRO sensory neuron spike trains, which is facilitated by training in data analysis using python.

Key words: suction electrode, Arduino controller; rotary actuator, mechanotransduction; sensory coding; spike train analysis; neural adaptation; Procambarus clarkii

The muscle receptor organs (MROs) of decapod crustacea were introduced to neuroscience in 1951 (Alexandrowicz, 1951) and rapidly became favored material for a variety of types of analysis, including biophysical analysis of membrane currents (Eyzaguirre and Kuffler, 1955; Terzuolo and Bullock, 1956; Edwards and Ottoson, 1958; Terzuolo and Washizu, 1962; Loewenstein et al., 1963; Nakajima and Onodera, 1969; Sokolove and Cooke, 1971; Brown et al., 1978; Rydqvist, 2007; Purali, 2011, 2017), cellular analysis of synaptic inputs (Kuffler and Eyzaguirre, 1955; Burgen and Kuffler, 1957) and outputs (Macmillan and Vescovi, 1997; Nakagawa and Mulloney, 2001; Drummond and Macmillan, 2004) of the MRO sensory neurons, and circuit level analysis of reflex function during crayfish postural movements (Eckert, 1961b, 1961a; Fields and Kennedy, 1965; Fields, 1966; Fields et al., 1967; Page and Sokolove, 1972, 1973; Patullo et al., 2001; Faulkes and Macmillan, 2002; McCarthy et al., 2004). The anatomy and physiology of the crayfish MROs are in several regards analogous to mammalian muscle spindles (Knellwolf et al., 2019), which added to their popularity (Kuffler, 1954). The sensory neurons of the crayfish MRO were also central to the analysis of gamma-aminobutyric acid (GABA) and other neurotransmitters at the synapses onto the soma and dendrites of the MRO sensory neurons from efferent modulatory neurons (Wiersma et al., 1953; Florey, 1954; Kuffler and Edwards, 1958; Edwards and Kuffler, 1959; Hagiwara et al., 1960; Sokolove and Roth, 1978; Craelius and Fricke, 1981; Elekes and Florey, 1987). In addition, a variety of quantitative modeling and simulation studies provided insights into MRO functions at several levels of analysis, from biophysical to network (Brown and Stein, 1966; Sokolove, 1972; Hartline, 1976; Macmillan, 1990; Swerup and Rydqvist, 1996). Appreciation of the structure and function of the crayfish MROs was greatly aided by the elegant studies of Purali (2005). The crayfish stretch receptor preparation has been described for student use (Welsh et al., 1968b; Leksrisawat et al., 2010; Wyttenbach et al., 2014). Variations of this classic preparation (e.g., Khaitin et al., 2015) present opportunities for extending the student exercise.

Practice in the use of modern methods of data analysis requires the generation of data sets containing reproducible neural responses produced by systematic and quantitative variation of relevant stimulus parameters. For the crayfish MRO, this means manipulation of stretch speed and the extent of either transient or maintained stretch, preferably under software control. This stimulation method allows the clearest differentiation of the tonic (slowly adapting) MRO and the phasic (rapidly adapting) MRO. A readily constructed flexible suction electrode also is required to maintain good contact with the MRO sensory nerve during vigorous abdominal movements. A device to impose reproducible and quantitative translational movements on the crayfish abdomen during recordings is also required. These two items will be described in the first two sections of this paper. Finally, a new version of the crayfish abdominal preparation is described which allows linear extensions rather than curling movements to be imposed on the isolated abdomen. Sensory nerve recordings generated by our students will be presented to show typical results of the novel methods we describe.

Our learning goals and objectives for this laboratory exercise are 3-fold: 1. To introduce students to the basic functions of a proprioceptor, including its stimulus/response and adaptation properties; 2. To introduce students to reproducible methods of obtaining a stimulus/response function from a single sensory neuron; 3. To introduce students to the concept of quantitative analysis of neuronal responses for application to multiple identical stimuli.

MATERIALS AND METHODS

Novel suction electrode design

To record from the MRO sensory nerve, we use a visually controlled fracture of a glass microelectrode that is directly coupled to a 1 mL syringe and suction tubing with a Tuohy adapter. The syringe body allows the electrode to be mounted on a coarse micromanipulator (Sutter MM-33 or equivalent). We prepare the glass suction electrode tips, silver wires, and suction apparatus, and the students assemble the working suction electrode from these components. Production of the suction electrode tips and apparatus is described detail in Appendices B and C.

The glass suction electrode tip is broken from a long glass microelectrode (pulled from capillaries of OD 1.2 mm, Sutter B120-69-15), using a serrated ceramic tile, at a diameter appropriate to hold the cut end or a loop of the MRO nerve (generally 150-300 µm). A chlorided silver wire is inserted into the lumen of the glass microelectrode and a second chlorided silver wire is affixed to the outside of the electrode near the tip (Figure 1A). The glass microelectrode is coupled to a 1mL syringe with a Tuohy adapter (1510, S4J Manufacturing Services, Inc., Cape Coral, FL), and the syringe is connected via silastic tubing to a suction apparatus (Figure 1B, 1C). Suction is imposed with a 10mL syringe and a 4-way Luer stopcock.

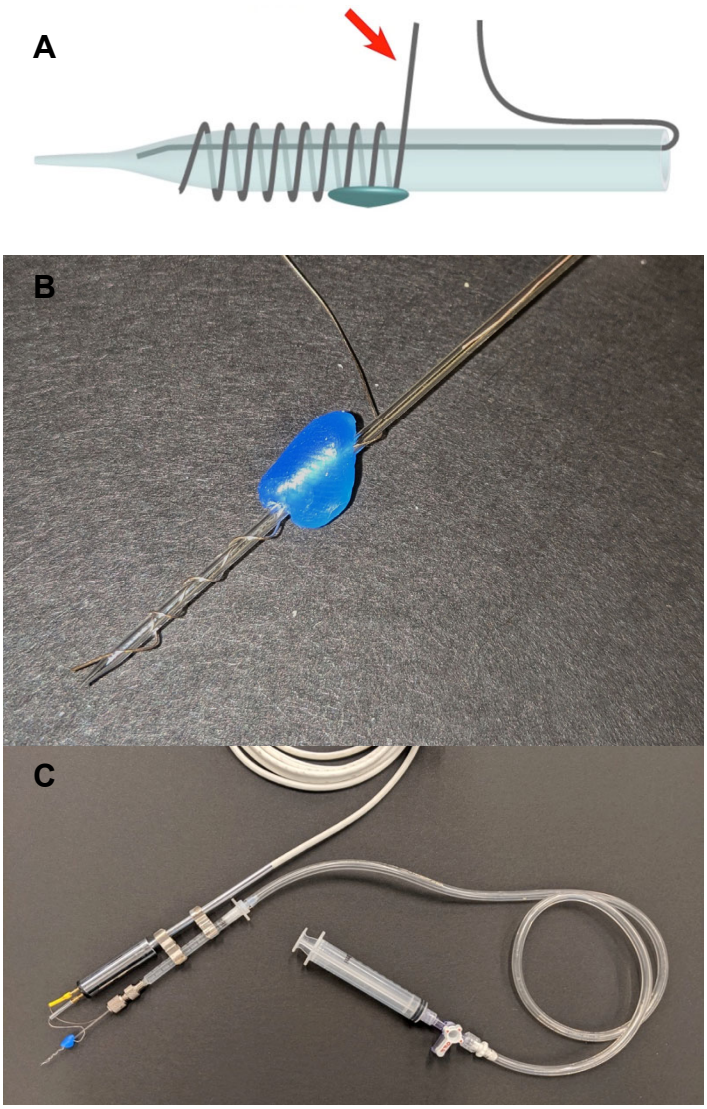

Figure 1. A. Diagram to show the layout of the two silver wires, one inside and one outside the tip of the suction electrode. The outer silver wire (red arrow) is shown stabilized to the outside of the suction electrode tip with a small piece of dental wax. *B.* Magnified view of assembled suction electrode tip. Note that the inside wire does not extend to the electrode tip; it needs only a fluid column in contact with the saline bath to function. *C.* Example of a fully assembled suction electrode.

Arduino controlled MRO stimulator

To achieve quantitative and reproducible activation of the MRO sensory cells, we have developed an Arduino-controlled rotary actuator which at maximum speed and translation distance can reliably activate both the phasic and tonic MRO neurons during imposed curls of the abdomen (Figure 2). Slow speeds and short distances are sufficient to activate the tonic MRO neurons alone, while the phasic MRO neuron can be recruited at higher speeds and longer distances. The rotary actuator design was chosen after an initial design with a linear actuator was unable to generate the displacement speed necessary to activate the phasic MRO neuron. The maximum speed achieved by the rotary actuator is >1000 mm/sec.

The apparatus is designed such that a rotary actuator in the form of a servo motor (DaViga DS213, Aloft Hobbies, Novato, CA) gives approximately linear displacement to an attached flexible wire when moving over a 90° sweep of its arc. The technical specifications for the DaViga DS213 are given in Appendix VIII. The rotary position of the servo is controlled by an Arduino (Arduino Uno R3, Sparkfun: https://www.sparkfun.com). The Arduino board and servo motor are mounted in a compact plastic housing (LH43-200 kit, PacTec, Concordville, PA), which is securely connected to a 7 mm diameter aluminum rod to simplify mounting the device on a coarse micromanipulator. The device also has a BNC connector which outputs a position signal to be recorded simultaneously with the electrode recording. A loop in the end of the flexible wire that emerges from the device housing is connected to a strong thread that is tied to the telson of the crayfish abdomen. The apparatus housing is mounted in a coarse micromanipulator and positioned so that the baseline level of tension applied to the MRO is set by the X-axis control of the coarse micromanipulator. The puller is supplied to the students preassembled in an enclosed case. The interior of the apparatus is shown in Figure 2, and device schematics are shown in Appendix VII.

The Arduino board is flashed with a script using the standard servo library. The Arduino takes serial commands over a USB connection, generated from a graphical user interface (GUI) on the student's computer. This GUI, written in python, allows the student to control the linear extent and speed of retraction, and allows for repeated trials with a given set of stimulus parameters. These controls are sufficient for precise and reproducible stimulation as presented in this manuscript, and students seeking more intricate stimulus timing or parameters can edit or create

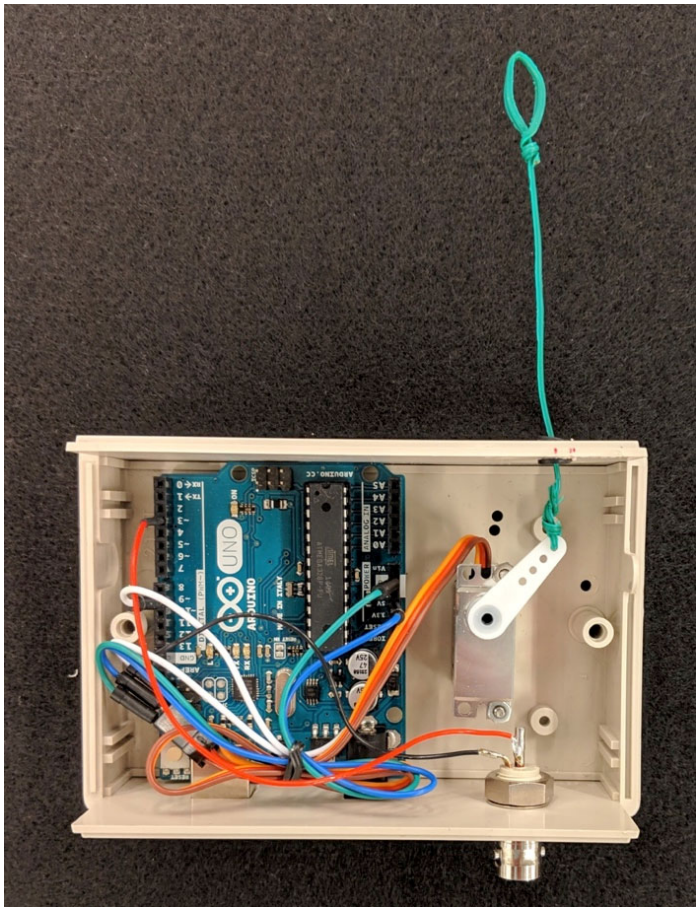

Figure 2. Interior view of the Arduino-controlled micro-rotary actuator shows the Arduino board mounted next to the rotary actuator, connections to the input and output ports, and the flexible wire attached to the actuator arm that exits the device housing. Device schematics are available in (Appendix VII).

new code to direct the action of the puller (e.g., sinusoidal patterns of stretch, to simulate patterns of activation during rhythmic swimming or tail flips). Code for the Arduino and GUI are available in Appendices I and J.

Preparation of the crayfish abdomen for activation of MRO by imposed movements

Tail curl

Preparation of a crayfish tail for stimulation of MROs by tail curling is as described by Wyttenbach et al. (2014), which includes movies illustrating the various steps of the dissection. Immerse a crayfish in crushed ice for at least 20 minutes. Remove the crayfish from the ice when it is unresponsive and quickly separate the abdomen from the cephalothorax. Immediately place the cephalothorax in a freezer. Isolate the dorsal surface of the abdominal carapace by making two longitudinal cuts along the margins of the dorsal carapace, then peel the dorsal carapace away from the ventral surface. Remove the fast flexor and extensor muscles to reveal the ends of the MRO sensory nerves on each side of each abdominal segment. Near the end of the MRO sensory nerve it is comprised of three branches. The central branch contains the MRO sensory axons, as shown in Figure 8.

Make a hole in the telson, insert a coarse thread through the hole and tie it in place. The other end of this string will be connected to the loop in the end of the flexible wire emerging from the Arduino-controlled stimulator box. Finally, pin the crayfish abdomen dorsal side down in a sylgard-lined preparation dish by pinning only the most anterior segment of the abdomen. This will allow tension on the string tied to the telson to impose abdominal flexion. Cover the preparation with crayfish saline (205 mM NaCl, 5.4 mM KCl, 10 mM CaCl2, 2.6 mM MgCl2, 2 mM glucose, 2.3 mM NaHCO3, pH 7.4). To avoid collisions between the tail fan and the suction electrode, the lateral components of the tail fan can be removed.

Linear stretch

In the standard laboratory preparation, the phasic MRO nerve tends to respond only to very fast tail curl stimuli, with the result that it can be hard to recruit. When the phasic MRO nerve is stimulated, the necessarily brief stimulus tends to evoke only a very small number of spikes, making

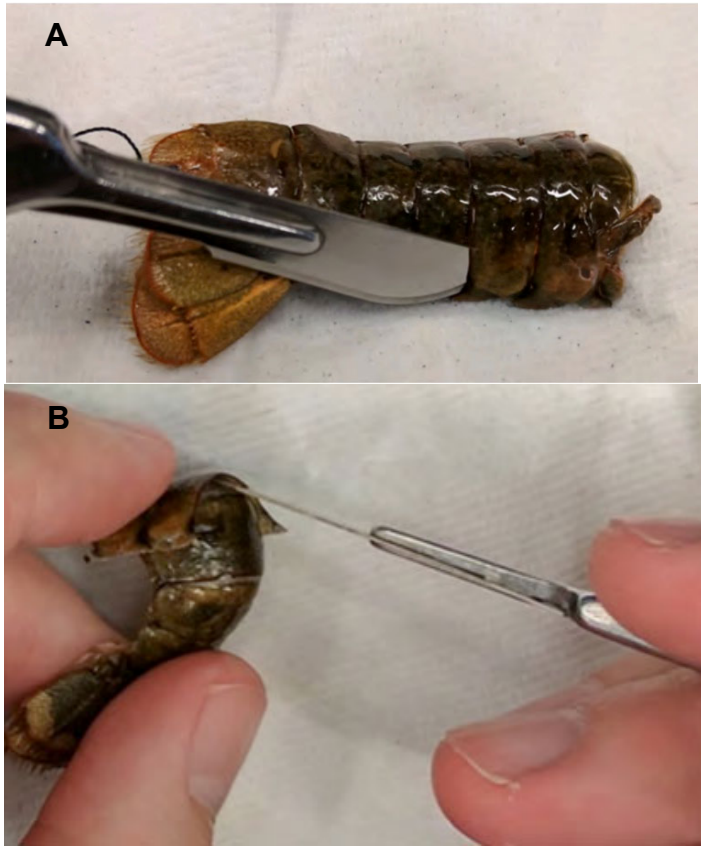

Figure 3. Dissection to separate two tail segments of the crayfish abdomen to allow excitation of MRO sensory neurons by linear extension of the abdomen. The segments are separated by cutting through the two hinge joints and the arthroidal membrane holding the segments together. *A.* Intersegmental hinge joints on either side are cut with the tail placed ventral side down on a firm surface. *B.* The arthroidal membrane should then be cut with the segment bent to 90 degrees, with the scalpel kept shallow and parallel to the more anterior segment, to prevent cutting the MRO or deep extensor muscles.

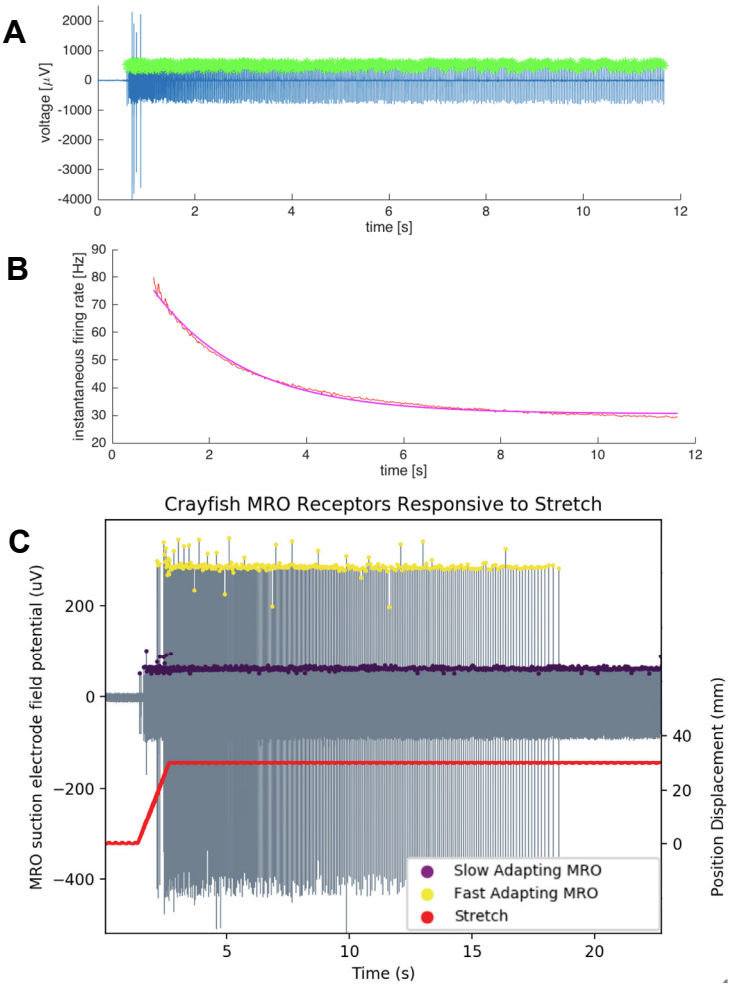

Figure 4. Example student recordings and analysis from the crayfish MRO nerve using the tail curl protocol described herein. *A.* A sample recording from the MRO sensory nerve showing responses from both the phasic MRO (larger, unlabeled spikes) and tonic MRO (smaller spikes with peaks labeled in green). *B.* An exponential model (magenta) (Wyttenbach et al., 2014; see Appendix I) fits the observed tonic MRO data (red) very well (R^2 = 0.994). *C.* A second example showing sustained responses from both the phasic and tonic MROs. In this example a 30 mm stretch at a speed of 25 mm/sec sequentially recruits the phasic and tonic MROs. Phasic MRO spikes are denoted with yellow markers; tonic MRO spikes are denoted with purple markers; and the puller position signal is plotted in red.

quantitative analysis (e.g., of adaptation) very difficult. The prior section details methods aimed at increasing the reproducibility of recruiting the phasic MRO with a fast pull. Here we describe an additional dissection step that allows MROs in a given segment to be stretched linearly, allowing both a simpler measurement of the muscle stretch and an investigation of the behavior of the phasic MRO outside its normal physiological constraints. This added step can be challenging for students new to dissection, so we present it to our undergraduates as an alternate approach. Thus some of our students who opt to implement this technique do so on the second day of lab designated for the MRO experiment, after successfully obtaining an MRO recording with the standard method on day 1.

This alternative approach follows the normal dissection protocol of Wyttenbach et al. (2014) up to and including the removal of fast flexor muscles to expose the MRO nerves. Students then identify the segment with the best candidate (i.e., visibly intact and accessible) MRO nerves. This segment is separated from the one posterior to it by using a #10 scalpel blade to cut through the tergite joints and the arthroidal membrane between segments (Figure 3). The remaining muscles including the MROs can now be stretched by applying a pull to the tail fan in a posterior direction, reliably recruiting both the phasic and tonic MROs.

A diagram showing the complete setup of the crayfish abdomen, Arduino-controlled stimulator, suction electrode and input probe of the extracellular amplifier is shown in Appendix VI. Commercial sources for living crayfish are listed in Appendix V.

RESULTS

Using the protocol modifications outlined above, our students are able to generate recordings from the MRO

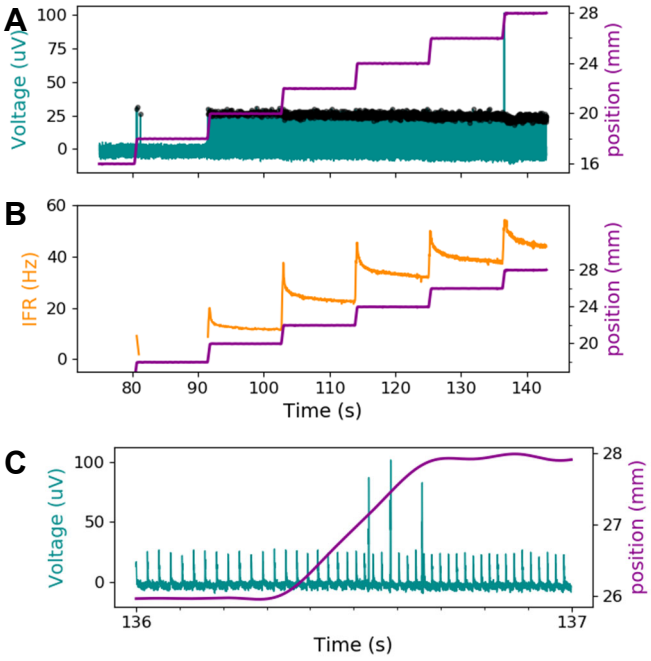

Figure 5. Student data demonstrating the tonic response to successive linear stretch stimuli and the stretch threshold of both tonic and phasic MRO units. The crayfish tail was prepared according to the protocol for linear stretch, and the tail was stretched in 2mm steps at minimum speed (5.25mm/s) while recording from the MRO nerve. *A.* The stretch applied revealed linear stretch thresholds for the tonic and phasic MROs. The initial threshold stimulus of the tonic MRO (cyan trace; tonic unit spikes labeled with black dots) happens near 18mm of linear stretch, and the unit ceases firing as it adapts to the first suprathreshold stimulus. The phasic MRO is recruited at a stretch distance of 26-28 mm. Position signal shown in purple. *B.* Instantaneous firing rate of the tonic MRO (orange traces) together with position signal (purple trace). Successive stretches show increasingly high initial and adapted firing rates. *C.* Magnified view of the recording shown in panel A, highlighting the recruitment of phasic MRO spikes at 27 mm of linear stretch.

nerve with reproducible, user-varied stimuli, which offers the adapts from an initial firing rate to a steady state firing rate opportunity for more robust quantitative measurements and analysis. Sample student recordings of MRO sensory neuron activity in response to imposed abdominal curling or stretch according to these protocols are shown in Figures 4 and 5. Figure 4A shows the most typical response profile of the MRO nerve: after a tail curl, the tonic MRO over 10 seconds, and can be modeled with an exponential decay function (Figure 4B; Appendix I). The phasic MRO (generally a much larger unit) responds during the fast pull with a burst that is too abrupt to fit to an exponential. Figure 4C captures a rare, sustained phasic MRO response at maximum tail curl, a feature we were aiming to capture reliably in the development of the linear stretch approach to dissection. Data from the linear stretch preparation are shown in Figure 5, in an exploration of responses at successive stretch distance, including a phasic MRO response despite the slow stimulus speed.

The utility of reproducible stimulation of the MRO is shown in Figures 6 and 7, in which a sequence of thirteen consecutive extensions is imposed in an investigation of the relationship between MRO adaptation and recovery time between stimuli. The rapidly delivered stimuli at maximal pull speed elicit short bursts from the phasic MRO neuron, and activity from the tonic MRO neuron that is sustained for the duration of the imposed flexion. In contrast to the tonic MRO, the phasic MRO does not recover to full responsiveness at the shortest rest intervals, most likely due to the dramatic differences in adaptation kinetics between the fast and slow MROs. This difference in adaptation of the two MRO units is quantified by fitting each stimulus response to an exponential decay curve (Figure 7 and Appendix I). The adaptation rate tau varies as a function of recovery time for the phasic MRO (Figure 7D), but initial and adapted firing rates do not vary as a function of rest time for either MRO. The ability to gather extensive data sets with reliable and reproducible mechanical stimuli applied to the RO sensory neurons while maintaining high quality recordings from the sensory nerve is the major advantage of using the Arduino-controlled device.

DISCUSSION

Course context

The MRO exercise is deployed in two neuroscience laboratory courses: a core lab for undergraduate neuroscience majors who generally take it in the spring semester of their junior year, and a core lab for first year neuroscience graduate students. Our teaching lab has a capacity for 16 students working in pairs; we generally run one section of the graduate course in the fall and two to three sections of the undergraduate lab in the spring. Both courses are open to students from other concentrations, and in recent years we have had visiting molecular biology, physics, and engineering students. The courses meet twice per week for laboratory sessions: 3 hours per session for the undergraduate course and 4 hours per session for the graduate course. In both courses, students submit figures each week, demonstrating a quantitative analysis of the data recorded in that week's module, as well as two lab reports over the course of the semester, which explore the experiments in greater depth. The second lab report is based on an independent project, designed and completed by students in the final two weeks of the semester. The

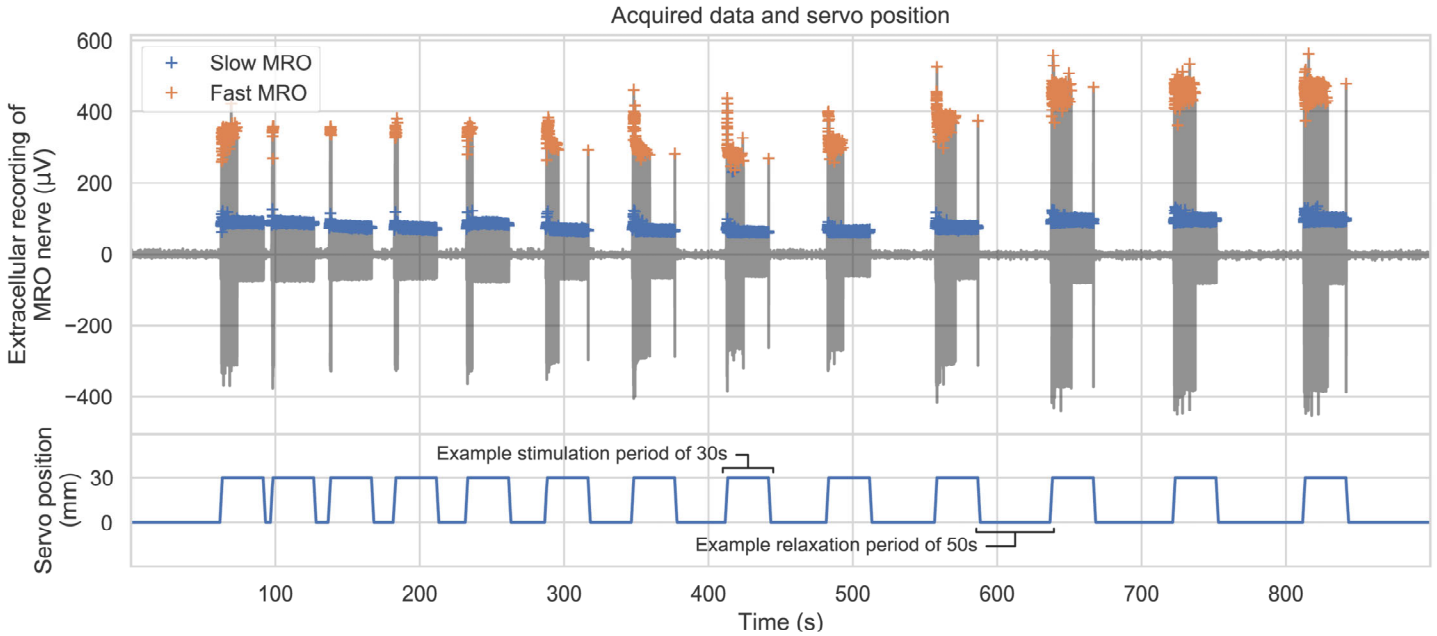

Figure 6. Student recording showing a sequence of Arduino-commanded MRO flexions delivered while both MRO sensory nerve activity and rotary actuator position signal are recorded, in an investigation of the relationship between adaptation rates and recovery time between trials. Upward deflections in the servo position trace indicate puller retraction (tail curl) and downward deflections indicate relaxation. The change in spike height is likely due to a change in suction electrode contact with the nerve.

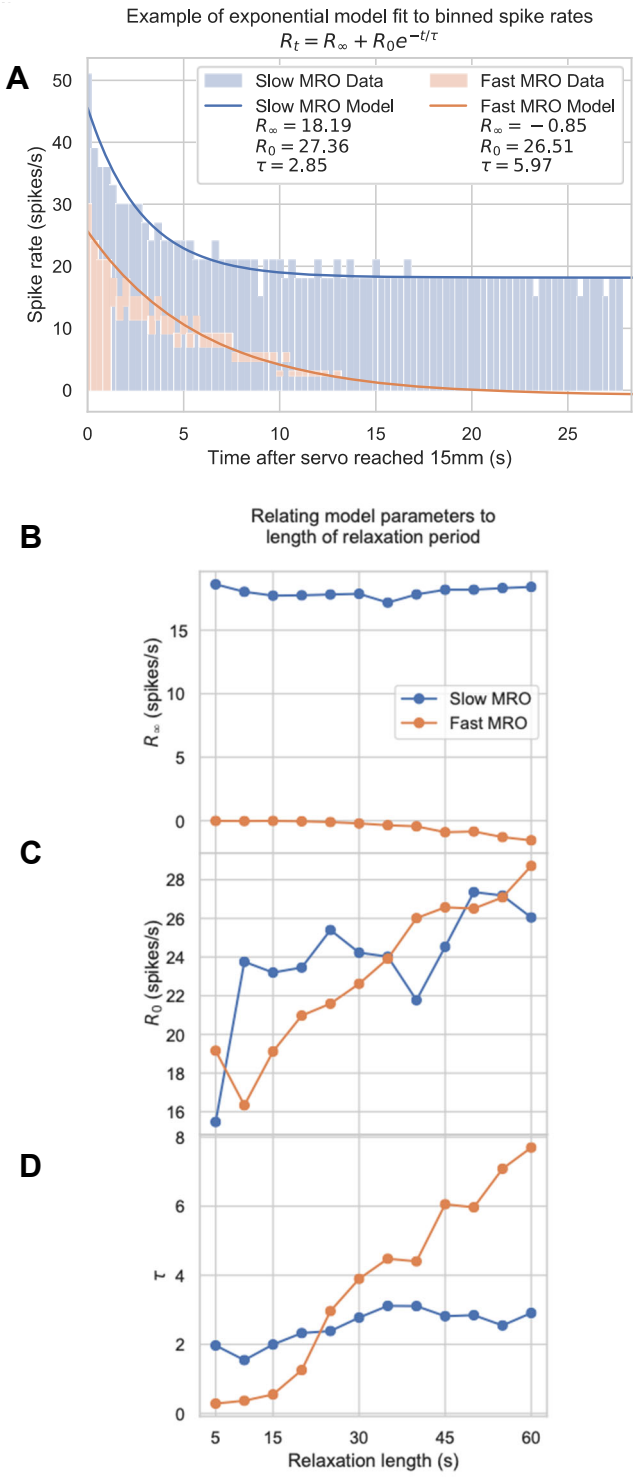

Figure 7. A. Binned spike rates and exponential model fits for the phasic and tonic MRO neurons during an extended stimulation period shown in Figure 6. Spike rate was modeled in python as an exponential function of time with form $R_t = R_\infty + R_0 e^{-t/\tau}$ (Wyttenbach et al., 2014; Appendix I). As expected, the phasic MRO ceased firing while the tonic MRO had a sustained response following adaptation. *B-D.* Plots of the fit parameters as a function of recovery time between stimuli. One interesting observation was that the firing rate decay (τ) was found to vary with the recovery time between trials for the phasic MRO but not the tonic MRO, with phasic MRO adapting more quickly at short recovery times.

student data presented in this paper are from these figure and lab report assignments. To alleviate the pressure to generate good data from challenging experiments on a weekly basis, we have an explicit data sharing policy, allowing free use of classmates' data with their permission and proper attribution.

Our feedback to the students on their assignments is spread between the quality of quantitative analyses and clarity in explaining those analyses (both visually and textually). We aim to structure each module so that students learn a laboratory technique, and then use that technique to ask a question of the system under study. To facilitate this we provide tutorial materials in the form of jupyter notebooks illustrating analysis of sample data using python. We frame this exercise in terms of sensory coding, and introduce (1) plotting of binned or instantaneous firing rate (IFR) and (2) curve fitting to the analysis 'toolbox', which includes data handling, plotting, peak detection, and amplitude-based spike sorting from earlier weeks. The student analyses for this exercise tend to focus either on comparing responses between different stimulus parameters they manipulated during data collection (speed, distance, recovery time) or a quantitative exploration of adaptation under a single stimulus mode. Students who don't wish to fit a decay curve can still compare initial and adapted firing rates and relative adaptation rates by manually inspecting their IFR plots.

This lab is the third module in our course and the first time our students are prompted to develop a question to ask about their data by choosing the conditions under which they wish to make their recordings. (The preceding two weeks of recording from the crayfish neuromuscular junction are more prescriptive in terms of experimental design.) The focus on framing a question at this stage firmly establishes that expectation going forward, and dispenses with questions about how to frame the empirical question *after* an experiment has been performed. The students have done well with this freedom, with some venturing outside the manipulations we suggest: we only added recovery time to our list of parameters to explore after a student submitted the analysis shown in Figures 6 and 7.

Some students struggle with the details involved in generating the figures at this stage. For example, occasionally students will fail to look closely enough at their data to exclude the tactile hair response in the analysis of the tonic MRO. (This arises from the fact that the MRO nerve includes a branch that receives sensory input from the exoskeleton, which can introduce movement-based artifacts; see Figure 8). We view these mistakes as the opportunity for the most learning to happen in the course, which we encourage with a robust feedback cycle, and reduce the sting of by making each figure a small part of the final grade (figures collectively being worth as much as one lab report). We find that our students' ability to generate effective figures improves over the course of the semester, and they report that this was the most generalizable skill they acquired from their experience in the course.

When we first developed this course, we presented parallel tutorial materials using either Matlab or, for students who did not wish to learn to code, Excel and the analysis

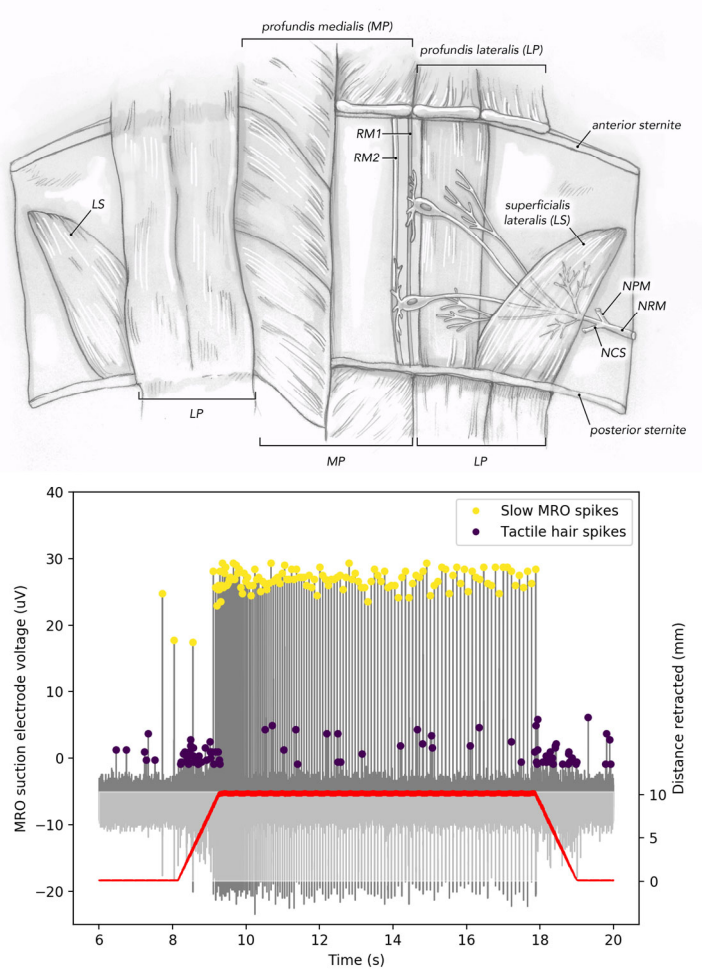

Figure 8. A. Semi-diagrammatic figure showing the three nerve branches that converge to form the main trunk of the MRO nerve. NPM = nerve to the profundis (deep extensor) muscles, NRM = nerve to the MROs, NCS = nerve to sensory hairs on the exoskeleton. RM1, RM2 = receptor muscle 1 and 2. Anterior is to the top of the panel. See Wiersma (1953) for further details. *B.* MRO recording from a tail curl experiment separating the tactile hair response (purple dots) from the tonic MRO response (yellow dots). Students may misidentify the tactile hair response as an MRO unit if they fail to pay attention to (or record) the release of tail stretch.

suite packaged with our acquisition software (Clampfit). Since that time the ubiquity of coding in neuroscience has made it inescapable in the context of our teaching lab. We have settled on python as the language of choice for our tutorial materials, but since programming literacy is generalizable, we require programming experience in any language as a prerequisite for the course, and students can perform their analysis using any language they choose. In the earliest phase of the course we hold supplementary office hours to help with the practical use of python for analysis of electrophysiology data. For students without a strong computational background, two useful references are (Cohen, 2017; Nylen and Wallisch, 2017).

MRO system

The sensory neurons of the crayfish MROs provide readily accessible preparations for the quantitative study and modeling of sensory transduction (Brown and Stein, 1966; Sokolove, 1972; Hartline, 1976; Macmillan, 1990; Swerup and Rydqvist, 1996) and neuromodulation, particularly the inhibitory input from GABAergic interneurons making synapses directly on the dendrites and somata of the MRO sensory neurons (Kuffler and Edwards, 1958; Edwards and Kuffler, 1959; Sokolove and Roth, 1978; Craelius and Fricke, 1981). The properties of the crustacean MROs have been extensively reviewed (Alexandrowicz, 1967; Swerup and Rydqvist, 1992; Rydqvist, 2007; Rydqvist et al., 2007); however, many essential aspects of their biophysical properties and behavioral control functions remain to be elucidated, presenting a rich variety of opportunities to use this preparation in extending basic student exercises and formulating student research projects..

Stimulation of the isolated MRO sensory nerve while recording from the tonic MRO neuron intracellularly reveals antidromic stimulus-locked IPSPs for some stimulus strengths at some stimulating electrode positions (Sokolove and Cooke, 1971). The peripheral axons of the GABAergic efferent neurons presumably maintained their viability in these experiments (Bittner, 1991). These stimulus-evoked IPSPs are likely to be due to the GABAergic efferent synapses onto the MRO sensory neurons. The study of the reflex activity patterns in efferent neurons making synapses on the MRO sensory neurons will be facilitated by a recently-described version of the crayfish abdominal MRO preparation which maintains its central connections to the chain of abdominal ganglia (Khaitin et al., 2015).

The biophysical understanding of the ionic events underlying adaptation in the crayfish MROs has focused on the ability of stretch-sensitive channels in the MRO membranes. The stretch-activated channels mediate adaptation of the receptor current by admitting calcium ions which act internally to activate a potassium current responsible for the fast phase of receptor current adaptation (Erxleben, 1989, 1993; Rydqvist et al., 2007). Presumably the fast and slow MROs differ in the number and sensitivity of the stretch-activated channels and the kinetics of activation of the calcium-sensitive potassium channels.

A leading candidate for the deformation-sensitive MRO sensory neuron membrane channels is one or more of the newly described mechanosensitive piezo family of ion channels (Woo et al., 2015; Haselwandter and MacKinnon, 2018; Zhao et al., 2018). Piezo channels have been shown to be essential for stretch-activated mechanical transduction in the larval Drosophila dorsal bipolar dendritic sensory neurons (Suslak et al., 2015). Also, some progress has been made in understanding the substructure of the piezo channels and the molecular features important for stretch activation (Lacroix et al., 2018). This molecular information may allow creation of a more selective piezo channel blocker than gadolinium (Swerup et al., 1991) or tarantula toxin GsMTx4 (Bowman et al., 2007; Bae et al., 2011; Lee et al., 2014) which can then be applied to the crayfish MRO sensory neurons to confirm or refute the hypothesis that piezo channels are required for MRO sensory neuron responses to stretch (McCubbin et al., 2020).

The crayfish abdominal posture control system, of which

the MRO sensory neurons are presumably an integral part, mediates both slow adjustments of abdominal extension and flexion, and fast movements during repetitive tail flips that mediate escape swimming. It has been remarkably difficult to demonstrate robust effects on either of these two motor outputs due to ablation of the MROs or correlate MRO activity during behavior by recording their activity during spontaneous or stimulus-evoked abdominal movements (Patullo et al., 2001; Faulkes and Macmillan, 2002; McCarthy et al., 2004). It may require dual site recording with implanted cuff electrodes on the MRO sensory nerve to distinguish afferent and efferent axon activity during both fast and slow abdominal postural changes. Another important aspect of these studies of the MRO activity in situ is whether or not abdominal movements are working against an opposing force (Page, 1978; Sukhdeo and Page, 1992). Also, it is important to realize that there is a second set of stretch sensitive sensory neurons in the crayfish abdomen, mediated by stretch receptors in the ventral nerve cord itself (Grobstein, 1973a; 1973b; Savati and Macmillan, 1993; Drummond and Macmillan, 2002). These crayfish nerve cord stretch receptors are analogous to stretch receptors described in abdominal nerves of Phormia that play a critical role in the regulation of food intake (Gelperin, 1971). The role of the crayfish nerve cord stretch receptors in postural control of the abdomen is unknown, although description of the ultrastructure of the phasic nerve cord stretch receptor (Cobb and Heitler, 1985) may offer some guidance as to its function.

Previous work using an electrically activated stretch stimulus to the MRO spanning the cephalothorax-abdomen junction allowed application of periodic stimulus variations such as sine waves or ramp variations in stretch to be applied during tonic firing of the slow adapting MRO sensory cell (Vibert et al., 1979). This MRO preparation also allowed intercalation of inhibitory input to the tonic sensory cell by electrical stimulation applied in the vicinity of the rapidly adapting phasic sensory cell. The electrical stimulus activated the fibers of an inhibitory neuron, resulting in inhibitory input to the tonic sensory cell by axon reflex (Nja and Walloe, 1975). In preparations retaining the connections of the MROs and the central ganglia, activation of two efferent inhibitory fibers to the MRO sensory cells can be evoked by imposed activity in the MRO sensory cells themselves (Eckert, 1961b; Jansen et al., 1970a, 1970b; Jansen et al., 1971). The two MRO sensory cells on each side of each abdominal segment receive a total of four efferent inhibitory neurons (Wine and Hagiwara, 1977; Drummond and Macmillan, 1998a, 1998b). Understanding the reflex activation and dynamics of this population of efferent inhibitory neurons is critical to a complete description of MRO function in vivo.

Suction electrode design

The fabrication and use of a variety of suction electrodes have been described (Easton, 1960, 1965; Kanno, 1963; Florey and Kriebel, 1966; Welsh et al., 1968a; Brown et al., 2006) including versions particularly suited to use in a teaching laboratory (Easton, 1993; Land et al., 2001; Johnson et al., 2007). A very useful feature of the suction electrode design described here is the ability to quickly and easily change electrode tips to optimize the snug fit of a nerve end or nerve loop in the electrode tip. Theoretical studies of suction electrode recording configurations (Stys et al., 1991; Easton, 1993) emphasize the importance of reducing leakage of action currents around the exterior of the nerve in the electrode tip to achieve optimum signal to noise ratios in the recorded signals. The suction electrode configuration we describe here can work with very small tip openings (5 – 10 µm ID) which proved critical for recording from a very small insect nerve, the recurrent nerve of the blowfly Phormia regina (Gelperin, 1967).

Learning to assemble their own suction electrodes is an important component of this laboratory exercise, as the students learn that they are recording the potential difference between points (the inner and outer wires of the suction electrode); and that when a length of active nerve is lodged in the suction electrode's tip, the recording pathway includes the extracellular space around the axons in the nerve, which is where local currents flow during the passage of an action potential. They also learn the importance of the nerve in the electrode tip making a snug fit and have the ability to easily change the glass electrode tip to find a tip of optimal size for the nerve from which they are aiming to record.

A recent innovation in techniques for in vivo recording involves application of microfabrication methods to the design and construction of implanted microelectrodes. This fabrication method has allowed significant progress in the ability to make in vivo recordings from crayfish nerve fibers (Lott and Hoy, 2008; Chen et al., 2009). Silicone encapsulated pairs of hook electrodes have also been used to record afferent and efferent activity in vivo from the dorsal branch of nerve 2 in the crayfish abdomen during both postural adjustment, walking and tail flips (Gruhn and Rathmayer, 2002).

Arduino Mechanostimulator

Arduino microcontrollers are increasingly popular for controlling and sensing applications in the neuroscience laboratory, as they are inexpensive open-source devices supported by an extensive user community (Teikari et al., 2012; Sheinin et al., 2015; Artoni et al., 2016; Landa-Jimenez et al., 2016). Arduinos incorporate communication via a USB port that serves both to provide power to the board and for uploading control programs, either custom written or from a standard library. Arduino boards are equipped with analog and digital input/output pins facilitating creation of control signals for external devices, such as an LED (Titlow et al., 2015) or the rotary actuator used in the MRO stimulation device described here. Free tutorials on the use of Arduino devices are readily available (www.arduino.cc/en/Tutorial).

CONCLUSIONS

The muscle receptor organs of the crayfish, Procambarus clarkii, provide a widely used and readily accessible preparation for the study of general principles of sensory

coding, particularly for mechanoreceptive stimuli. The pedagogical value of studies of this preparation is greatly enhanced by the ability to apply reproducible, quantitative stretch stimuli to the receptor muscles while recording the spike trains from the MRO sensory neurons elicited by these stimuli. The data sets generated by application of the mechanostimulator described here allow quantitative analysis of response reproducibility and the kinetics of response evolution with time after stimulus application, using readily available software tools. The combination of these factors greatly enhances the utility and effectiveness of student studies of the crayfish MRO preparation.

REFERENCES

Alexandrowicz JS (1951) Muscle receptor organs in the abdomen of Homarus vulgaris and Palinurus vulgaris. Q J Microsc Sci 92:163-199.

Alexandrowicz JS (1967) Receptor organs in thoracic and abdominal muscles of crustacea. Biol Rev 42:288-326.

Artoni P, Landi S, Sato SS, Luin S, Ratto GM (2016) Arduino Due based tool to facilitate in vivo two-photon excitation microscopy. Biomed Opt Express, 7(4):1604-1613.

Bae C, Sachs F, Gottlieb PA (2011) The mechanosensitive ion channel Piezo1 is inhibited by the peptide GsMTx4. Biochemistry, 50(29):6295-6300.

Bittner GD (1991) Long-term survival of anucleate axons and its implications for nerve regeneration. Trends Neurosci 14(5):188-193.

Bowman CL, Gottlieb PA, Suchyna TM, Murphy YK, Sachs F (2007) Mechanosensitive ion channels and the peptide inhibitor GsMTx-4: history, properties, mechanisms and pharmacology. Toxicon, 49(2):249-270.

Brown HM, Ottoson D, Rydqvist B (1978) Crayfish stretch receptor: an investigation with voltage-clamp and ion-sensitive electrodes. J Physiol 284:155-179.

Brown MC, Stein RB (1966) Quantitative studies on the slowly adapting stretch receptor of the crayfish. Kybernetik 3(4):175-185.

Brown TM, Banks JR, Piggins HD (2006) A novel suction electrode recording technique for monitoring circadian rhythms in single and multiunit discharge from brain slices. J Neurosci Methods 156(1-2):173-181.

Burgen AD, Kuffler SW (1957) Two inhibitory fibres forming synapses with a single nerve cell in the lobster. Nature 180:1490-1491.

Chen CH, Yao DJ, Tseng SH, Lu SW, Chiao CC, Yeh SR (2009) Micro-multi-probe electrode array to measure neural signals. Biosens Bioelectron 24(7):1911-1917.

Cobb JL, Heitler WJ (1985) Ultrastructure of the phasic stretch receptor in the crayfish abdominal nerve cord. J Neurocytol 14(3):413-426.

Cohen MX (2017) MATLAB for Brain and Cognitive Scientists. Cambridge, MA: MIT Press.

Craelius W, Fricke RA (1981) Release of 3H-gamma-aminobutyric acid (GABA) by inhibitory neurons of the crayfish. J Neurobiol 12(3):249-258.

DiStefano R, Litvan M, Meyer A, Taylor C (2008) Identifying crayfish: A guide for bait vendors and aquaculturists. In: (Conservation MDo, ed), pp 1 - 8. Jefferson City, MO: Missouri Department of Conservation.

Drummond JM, Macmillan DL (1998a) The abdominal motor system of the crayfish, Cherax destructor. II. Morphology and physiology of the deep extensor motor neurons. J Comp Physiol A 183:603-619.

Drummond JM, Macmillan DL (1998b) The abdominal motor system of the crayfish, Cherax destructor. I. Morphology and physiology of the superficial extensor motor neurons. J Comp Physiol A 183:583-601.

Drummond JM, Macmillan DL (2002) The cord stretch receptors in the abdominal nerve cord of the crayfish Cherax destructor: physiology and relationships. J Comp Physiol A Neuroethol Sens Neural Behav Physiol 188(5):349-357.

Drummond JM, Macmillan DL (2004) Morphology and connections of the abdominal accessory neurons of the crayfish Cherax destructor. J Comp Neurol 469(4):548-558.

Easton DM (1960) Nerve end recording in conducting volume. Science 132(3436):1312-1313.

Easton DM (1965) Impulses at the artifactual nerve end. Cold Spring Harb Symp Quant Biol 30:15-28.

Easton DM (1993) Simple, inexpensive suction electrode system for the student physiology laboratory. Am J Physiol 265(6 Pt 3):S35-46.

Eckert RO (1961a) Reflex relationships of the abdominal stretch receptors of the crayfish. II. Stretch receptor involvement during the swimming reflex. J Cell Comp Physiol 57:163-174.

Eckert RO (1961b) Reflex relationships of the abdominal stretch receptors of the crayfish. I. Feedback inhibition of the receptors. J Cell Comp Physiol 57:149-162.

Edwards C, Ottoson D (1958) The site of impulse initiation in a nerve cell of a crustacean stretch receptor. J Physiol 143(1):138-148.

Edwards C, Kuffler SW (1959) The blocking effect of gamma-aminobutyric acid (GABA) and the action of related compounds on single nerve cells. J Neurochem 4(1):19-30.

Erxleben C (1989) Stretch-activated current through single ion channels in the abdominal stretch receptor organ of the crayfish. J Gen Physiol 94(6):1071-1083.

Erxleben CF (1993) Calcium influx through stretch-activated cation channels mediates adaptation by potassium current activation. Neuroreport 4:616-618.

Elekes K, Florey E (1987) Immunocytochemical evidence for the GABAergic innervation of the stretch receptor neurons in crayfish. Neuroscience 22(3):1111-1122.

Eyzaguirre C, Kuffler SW (1955) Processes of excitation in the dendrites and in the soma of single isolated sensory nerve cells of the lobster and crayfish. J Gen Physiol 39(1):87-119.

Faulkes Z, Macmillan DL (2002) Effects of removal of muscle receptor organ input on the temporal structure of non-giant swimming cycles in the crayfish, Cherax destructor. Mar Freshw Behav Phy 35:149-155.

Fields HL (1966) Proprioceptive control of posture in the crayfish abdomen. J Exp Biol 44(3):455-468.

Fields HL, Kennedy D (1965) Functional role of muscle receptor organs in crayfish. Nature 206(990):1235-1237.

Fields HL, Evoy WH, Kennedy D (1967) Reflex role played by efferent control of an invertebrate stretch receptor. J Neurophysiol 30(4):859-874.

Florey E (1954) An inhibitory and an excitatory factor of mammalian central nervous system, and their action of a single sensory neuron. Arch Int Physiol 62(1):33-53.

Florey E, Kriebel ME (1966) A new suction-electrode system. Comp Biochem Physiol 18(1):175-178.

Gelperin A (1967) Stretch receptors in the foregut of the blowfly. Science 157(3785):208-210.

Gelperin A (1971) Abdominal sensory neurons providing negative feedback to feeding behavior of blowfly. Z Vergl Physiol 72:17-31.

Grobstein P (1973a) Extension-sensitivity in crayfish abdomen. 1. Neurons monitoring nerve cord length. J Comp Physiol 86:331-348.

Grobstein P (1973b) Extension-sensitivity in crayfish abdomen. 2. Tonic cord stretch reflex. J Comp Physiol 86:349-358.
Gruhn M, Rathmayer W (2002) An implantable electrode design for both chronic in vivo nerve recording and axon stimulation in freely behaving crayfish. J Neurosci Methods 118(1):33-40.
Hagiwara S, Kusano K, Saito S (1960) Membrane changes in crayfish stretch receptor neutron during synaptic inhibition and under action of gamma-aminobutyric acid. J Neurophysiol 23:505-515.
Hartline DK (1976) Simulation of phase-dependent pattern changes to perturbations of regular firing in crayfish stretch receptor. Brain Res 110(2):245-257.
Haselwandter CA, MacKinnon R (2018) Piezo's membrane footprint and its contribution to mechanosensitivity. eLife 7:e41968.
Jansen J, Nja A, Ormstad K, Walloe L (1971) Inhibitory control of the abdominal stretch receptors of the crayfish. IV. Quantitative description of the central coupling of the accessory reflex. Acta Physiol Scand 81(4):484-491.
Jansen JK, Nja A, Walloe L (1970a) Inhibitory control of the abdominal stretch receptors of the crayfish. II. Reflex input, segmental distribution, and output relations. Acta Physiol Scand 80(4):443-449.
Jansen JK, Nja A, Walloe L (1970b) Inhibitory control of the abdominal stretch receptors of the crayfish. I. The existence of a double inhibitory feedback. Acta Physiol Scand 80(3):420-425.
Johnson BR, Hauptman SA, Bonow RH (2007) Construction of a simple suction electrode for extracellular recording and stimulation. J Undergrad Neurosci Educ 6(1):A21-26.
Kanno T (1963) Electrical activity of the atrioventricular conducting tissue of the toad, studied by a minute suction electrode. Jpn J Physiol 13:97-111.
Khaitin AM, Rudkovskii MV, Uzdensky AB (2015) The method of isolation of the crayfish abdominal stretch receptor maintaining a connection of the sensory neuron to the ventral nerve cord ganglion. Invert Neurosci 15(1):176.
Knellwolf TP, Burton AR, Hammam E, Macefield VG (2019) Firing properties of muscle spindles supplying the intrinsic foot muscles of humans in unloaded and freestanding conditions. J Neurophysiol 121(1):74-84.
Kuffler SW (1954) Mechanisms of activation and motor control of stretch receptors in lobster and crayfish. J Neurophysiol 17(6):558-574.
Kuffler SW, Eyzaguirre C (1955) Synaptic inhibition in an isolated nerve cell. J Gen Physiol 39(1):155-184.
Kuffler SW, Edwards C (1958) Mechanism of gamma aminobutyric acid (GABA) action and its relation to synaptic inhibition. J Neurophysiol 21(6):589-610.
Lacroix JJ, Botello-Smith WM, Luo Y (2018) Probing the gating mechanism of the mechanosensitive channel Piezo1 with the small molecule Yoda1. Nat Commun 9(1):2029.
Land BR, Wyttenbach RA, Johnson BR (2001) Tools for physiology labs: an inexpensive high-performance amplifier and electrode for extracellular recording. J Neurosci Methods 106(1):47-55.
Landa-Jimenez MA, Gonzalez-Gaspar P, Perez-Estudillo C, Lopez-Meraz ML, Morgado-Valle C, Beltran-Parrazal L (2016) Open-box muscle-computer interface: introduction to human-computer interactions in bioengineering, physiology, and neuroscience courses. Adv Physiol Educ, 40(1):119-122.
Lee W, Leddy HA, Chen Y, Lee SH, Zelenski NA, McNulty AL, Wu J, Beicker KN, Coles J, Zauscher S, Grandl J, Sachs F, Guilak F, Liedtke WB (2014) Synergy between Piezo1 and Piezo2 channels confers high-strain mechanosensitivity to articular cartilage. Proc Natl Acad Sci USA 111(47):E5114-22.
Leksrisawat B, Cooper AS, Gilberts AB, Cooper RL (2010) Muscle receptor organs in the crayfish abdomen: A student laboratory exercise in proprioception. J Vis Exp 45:e2323.
Loewenstein WR, Terzuolo CA, Washizu Y (1963) Separation of transducer and impulse-generating processes in sensory receptors. Science 142(3596):1180-1181.
Lott GK 3rd, Hoy RR (2008) A polyimide pressure-contact multielectrode array for implantation along a submillimeter neural process in small animals. IEEE Trans Biomed Eng 55(6):1728-1732.
Macmillan DL (1990) The Crayfish Muscle Receptor Organ (MRO):- Model for the Membrane, Receptor, Circuit, and Behavioural Levels. In: Advancers in Life Sciences: Frontiers in Crustacean Neurobiology (Wiese K, Krenz WD, Tautz J, Reichert H, Mulloney B, eds) pp 75-82. Basel, Switzerland: Birkhäuser. Available at https://doi.org/10.1007/978-3-0348-5689-8_7.
Macmillan DL, Vescovi PJ (1997) Muscle receptor organs of the crayfish, Cherax destructor: Organisation of central projections of stretch receptor neurons. J Exp Zool 279(3):243-253.
McCarthy B, Daws A, Macmillan DL (2004) The activity of abdominal stretch receptors during non-giant swimming in the crayfish Cherax destructor and their role in hydrodynamic efficiency. J Comp Physiol 190(4):291-299.
McCubbin S, Jeoung A, Waterbury C, Cooper RL (2020) Pharmacological profiling of stretch activated channels in proprioceptive neurons. Comp Biochem Physiol C Toxicol Pharmacol, 233:108765.
Nakagawa H, Mulloney B (2001) Local specification of relative strengths of synapses between different abdominal stretch-receptor axons and their common target neurons. J Neurosci 21(5):1645-1655.
Nakajima S, Onodera K (1969) Adaptation of the generator potential in the crayfish stretch receptors under constant length and constant tension. J Physiol 200(1):187-204.
Nja A, Walloe L (1975) Reflex inhibition of the slowly adapting stretch receptors in the intact abdomen of the crayfish. Acta Physiol Scand 94(2):177-183.
Nylen EL, Wallisch P (2017) Neural Data Science A Primer with MATLAB and Python. San Diego, CA: Academic Press.
Page CH (1978) Load compensation in crayfish abdomen. J Comp Physiol 123:349-356.
Page CH, Sokolove PG (1972) Crayfish muscle receptor organ: Role in regulation of postural flexion. Science 175(4022):647-650.
Patullo BW, Faulkes Z, Macmillan DL (2001) Muscle receptor organs do not mediate load compensation during body roll and defense response extensions in the crayfish Cherax destructor. J Exp Zool 290(7):783-790.
Purali N (2005) Structure and function relationship in the abdominal stretch receptor organs of the crayfish. J Comp Neurol 488(4):369-383.
Purali N (2011) Antidromic potential spread modulates the receptor responses in the stretch receptor neurons of the crayfish. Pflugers Arch 462(6):821-834.
Purali N (2017) Fast calcium transients translate the distribution and conduction of neural activity in different regions of a single sensory neuron. Invert Neurosci 17(3):7.
Rydqvist B (2007) Ion channels for mechanotransduction in the crayfish stretch receptor. Curr Top Membr 59:21-48.
Rydqvist B, Lin JH, Sand P, Swerup C (2007) Mechanotransduction and the crayfish stretch receptor. Physiol Behav 92(102):21-28.
Savati F, Macmillan DL (1993) Physiology and morphology of the cord stretch receptors of the crayfish *Cherax destructor*. J Exp Zool 265(4):438-447.
Sheinin A, Lavi A, Michaelevski I (2015) StimDuino: an Arduino-based electrophysiological stimulus isolator. J Neurosci

Methods, 243:8-17.
Sokolove PG (1972) Computer simulation of after-inhibition in crayfish slowly adapting stretch receptor neuron. Biophys J 12(11):1429-1451.
Sokolove PG (1973) Crayfish stretch receptor and motor unit behavior during abdominal extensions. J Comp Physiol 84:251-266.
Sokolove PG, Cooke IM (1971) Inhibition of impulse activity in a sensory neuron by an electrogenic pump. J Gen Physiol 57(2):125-163.
Sokolove PG, Roth SH (1978) Effect of harmaline on the crayfish stretch receptor: blockade at a GABA-mediated inhibitory synapse. Neuropharmacology 17(9):729-735.
Stys PK, Ransom BR, Waxman SG (1991) Compound action potential of nerve recorded by suction electrode: a theoretical and experimental analysis. Brain Res 546(1):18-32.
Sukhdeo SC, Page CH (1992) Abdominal postural motor responses initiated by the muscle receptor organ in lobster depend upon centrally generated motor activity. J Exp Biol 162:167-183.
Suslak TJ, Watson S, Thompson KJ, Shenton FC, Bewick GS, Armstrong JD, Jarman AP (2015) Piezo Is essential for amiloride-sensitive stretch-activated mechanotransduction in larval Drosophila dorsal bipolar dendritic sensory neurons. PloS one 10(7):e0130969.
Swerup C, Purali N, Rydqvist B (1991) Block of receptor response in the stretch receptor neuron of the crayfish by gadolinium. Acta Physiol Scand, 143(1):21-26.
Swerup C, Rydqvist B (1992) The abdominal stretch-receptor organ of the crayfish. Comp Biochem Phys A 103(3):423-431.
Swerup C, Rydqvist B (1996) A mathematical model of the crustacean stretch receptor neuron. Biomechanics of the receptor muscle, mechanosensitive ion channels, and macrotransducer properties. J Neurophysiol 76(4):2211-2220.
Teikari P, Najjar RP, Malkki H, Knoblauch K, Dumortier D, Gronfier C, Cooper HM (2012) An inexpensive Arduino-based LED stimulator system for vision research. J Neurosci Methods, 211(2):227-236.
Terzuolo CA, Bullock TH (1956) Measurement of imposed voltage gradient adequate to modulate neuronal firing. Proc Natl Acad Sci U S A 42(9):687-694.
Terzuolo CA, Washizu Y (1962) Relation between stimulus strength, generator potential and impulse frequency in stretch receptor of Crustacea. J Neurophysiol 25:56-66.
Titlow JS, Johnson BR, Pulver SR (2015) Light activated escape circuits: A behavior and neurophysiology lab module using Drosophila optogenetics. J Undergrad Neurosci Educ 13(3):A166-A173.
Vibert JF, Davis M, Segundo JP (1979) Recurrent inhibition: its influence upon transduction and afferent discharges in slowly-adapting stretch receptor organs. Biol Cybern 33(3):167-178.
Welsh JH, Smith RI, Kammer AE (1968a) Electrophysiological equipment and techniques. In: Laboratory Exercises in Invertebrate Physiology, pp 198-209. Minneapolis, MN: Burgess Publishing Co.
Welsh JH, Smith RI, Kammer AE (1968b) Stretch receptors of the crayfish. In: Laboratory Exercises in Invertebrate Physiology, pp 85-87. Minneapolis, MN: Burgess Publishing Co.
Wiersma CAG, Furshpan E, Florey E (1953) Physiological and pharmacological observations on muscle receptor organs of the crayfish, Cambarus clarkii Girard. J Exp Biol 30:136-150.
Wine JJ, Hagiwara G (1977) Crayfish escape behavior: I. Structure of efferent and afferent neurons involved in abdominal extension. J Comp Physiol 121:145-172.
Woo SH, Lukacs V, de Nooij JC, Zaytseva D, Criddle CR, Francisco A, Jessell TM, Wilkinson KA, Patapoutian A (2015) Piezo2 is the principal mechanotransduction channel for proprioception. Nat Neurosci 18(12):1756-1762.
Wyttenbach RA, Johnson BR, Hoy RR (2014) Crawdad: An Online Lab Manual for Neurophysiology. Cary, NC: Sinauer Associates Oxford University Press.
Zhao Q, Zhou H, Chi S, Wang Y, Wang J, Geng J, Wu K, Liu W, Zhang T, Dong MQ, Wang J, Li X, Xiao B (2018) Structure and mechanogating mechanism of the Piezo1 channel. Nature 554(7693):487-492.

Received August 23, 2019; revised December 2, 2019; accepted July 25, 2020.

We thank William Dix and Stanley Chidzik of the Princeton Physics Department and James Plastine for help in the design and fabrication of the Arduino control box and students in NEU501B and NEU350 courses at Princeton University for sharing their experiences with these methods and devices, particularly Moritz Buchholz, Mona Clappier, Carlos Correa, Cameron Hayes, Sabrina Marques, and Deztynee Rivera, whose work is shown here. We thank Virginia Fulford for Figure 8A and Michael Kaplan for Figure 1A.

Address correspondence to: Alan Gelperin, Princeton Neuroscience Institute A75, Princeton University, Princeton, NJ 08544. Email: gelperin@princeton.edu

APPENDIX I
FITTING AN MRO FIRING RATE CURVE TO AN EXPONENTIAL DECAY EQUATION

The adaptation curve of MRO activity can be fit to an exponential of the form:

$$R_t = R_0 \cdot e^{-t/\tau} + R_\infty$$

In this equation, R_t is the firing rate at time t, R_∞ is the steady state firing rate; $R_0 + R_\infty$ is initial firing rate; and $1/\tau$ *(tau)* is the decay constant. Students should fit the binned or instantaneous firing rate curves beginning from the peak firing rate, using a utility like the *curve_fit* method from python's scipy package. The output will be the values for the three parameters (R_0 , R_∞ , and τ) that best fit the supplied data to the above equation. Fitting time-binned data can produce a more "visually satisfying" fit than IFR data when the decay is relatively fast, because the curve fitting is biased toward the part of the curve with a higher density of data points. Time binning reduces this bias, but in doing so loses resolution at the peak firing rate.

Students can make meaningful comparisons of initial and adapted firing rates and adaptation rates without curve fitting by comparing IFR curves plotted on the same axis. Initial and adapted firing rates can be estimated by eye, while the decay rate can be described as the time the curve takes to decay halfway to R_∞.

Having students fit the MRO response to this equation was described in Wyttenbach et al, 2014.

APPENDIX II
PREPARATION OF SUCTION ELECTRODE TIP

1. Pull a microelectrode blank as for a crayfish muscle intracellular recording electrode (Wyttenbach et al., 2014). We use 15 cm glass capillaries (Sutter B120-69-15) to create tips that are long enough to minimize complications caused by the crayfish telson hitting the electrode.
2. Under the low power of a dissecting microscope, score the tip of the microelectrode using a ceramic tile (CTS, Sutter Instruments, Novato, CA) so that when the tip is broken at the score, the inner diameter of the electrode tip makes a snug fit with the nerve end or with the nerve loop selected for recording. For recording from the end of the MRO sensory nerve the inner diameter of the tip of the suction recording electrode should be in the range 150 – 300 µm, depending on the size and species of the crayfish being used.
3. Two silver wires, 0.008" diameter and ~10cm length are soldered to connectors appropriate for the inputs to the head stage of the extracellular amplifier being used.
4. For most extracellular amplifiers, it will be useful to chloride the silver wires to avoid baseline drift. We use a 30 sec immersion of the ends of the silver wires in a ferric chloride PCB etchant solution (CAS No: 7705-08-0) to produce a sturdy layer of silver chloride. Use of this plating solution requires care to avoid skin contact and thorough rinsing of the plated silver wires to remove residual plating solution.
5. Fine stainless steel wires can be used in place of silver wires as a high pass filter on the amplifier input will block the offset potentials of the stainless steel wires. Note that in either case the bath ground wire must be a chlorided silver wire.

APPENDIX III
PREPARATION OF SUCTION ELECTRODE

The suction apparatus described here has a shelf life of several years, so long as they are stored without any residual crayfish saline. Saline left in the tubing will cause mold growth. An example of the completed suction electrode is shown in Figure 1B.

1. Drill out the back end of a 1 mL slip-tip BD disposable syringe (Cole Parmer UX-07944-00) using a drill size #3 or 7/32"
2. Use a ¼-28 tap to tap threads into the back end of the disposable syringe
3. Obtain a package of Loctite Plastics Bonding System with 4g Activator and 2g Adhesive
4. Obtain a PTFE adapter ¼-28 thread to 1/8" barb (DWK 953918-2313)
5. Apply the Loctite activator to the threads in both the syringe and on the adapter
6. Wait at least 1 minute for the activator solvent to evaporate
7. Apply Plastic Bonder Glue only to the threads on the adapter
8. Screw the adapter by hand firmly into the syringe and let dry for at least 1 day
9. Put a 32" length of Tygon tubing size 1/8" ID by ¼" OD (Cole Parmer EW-06407-76) onto the barbed fitting on the back end of the 1 mL syringe
10. Insert a 1/8" barb to female Luer (Cole Parmer EW-30800-08) adapter into the free end of the Tygon tubing
11. Mate the female Luer connection from the tubing to a male Luer-lock connection on a three-way stopcock (Mainlinemedical 9-5311-01)
12. Attach a 10 mL disposable BD slip-tip syringe (Cole Parmer UX-07944-14) to the female Luer connection on the stopcock opposite the tubing connection

Figure A1. Assembled suction electrode. Refer also to Figure 1 in the text.

APPENDIX IV
EQUIPMENT AND SOFTWARE DEPLOYED IN OUR TEACHING LAB

Equipment	Model	Manufacturer
extracellular amplifier	AM-3000	AM Systems (Everett, WA)
digitizer	Digidata 1440A	Molecular Devices (San Jose, CA)
acquisition software	pClamp/Clampex 10	Molecular Devices

APPENDIX V
COMMERCIAL SOURCES FOR LIVING CRAYFISH FOR BIOLOGICAL RESEARCH

1. Carolina Biological Supply, Burlington, NC	www.carolina.com
2. Ward's Science, Rochester, NY	www.wardsci.com
3. Nasco, Fort Atkinson, WI	www.enasco.com
4. Connecticut Valley Biological Supply, Southampton, MA	www.connecticutvalleybiological.com
5. Niles Biological, Sacramento, CA	www.nilesbio.com/

A very useful guide to identifying the species of crayfish that has been supplied is (DiStefano et al., 2008).

APPENDIX VI

Diagram showing the arrangement and electrode connections of the crayfish abdominal preparation, Arduino control box, suction electrode and amplifier input probe.

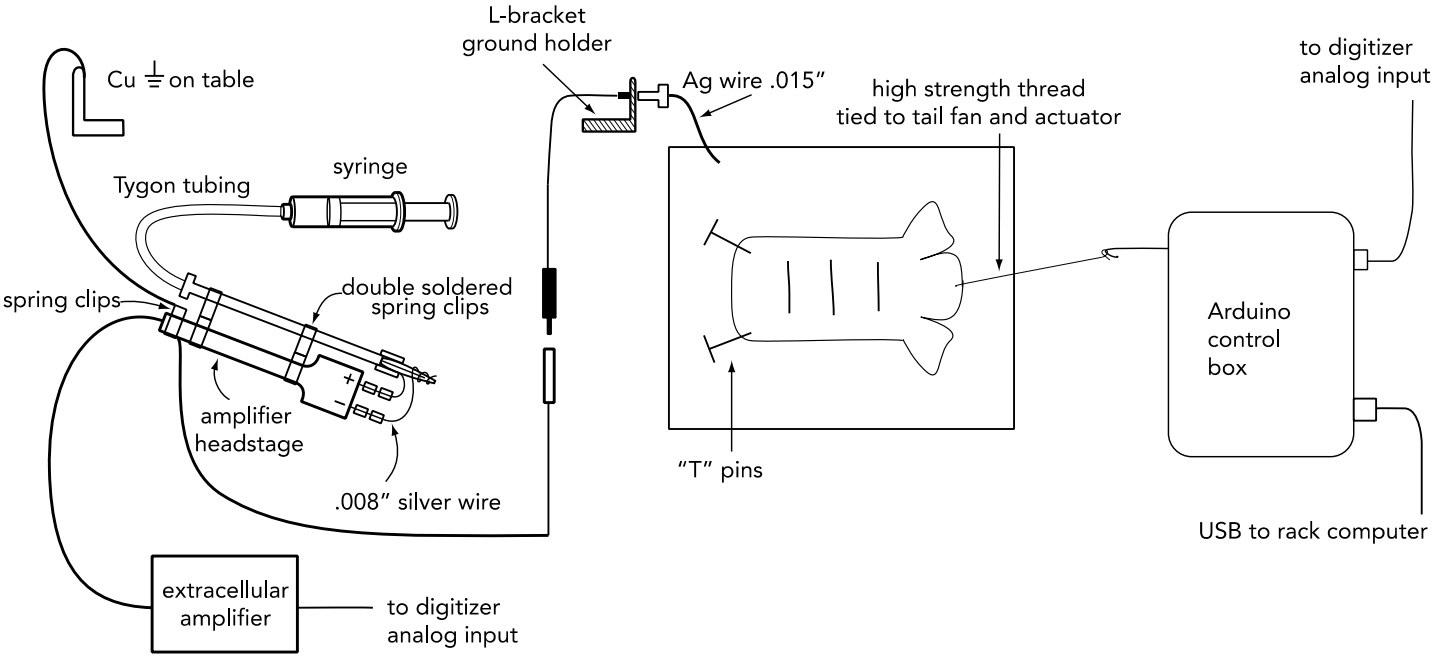

Figure A2. Diagram to show the arrangement and connections of the crayfish abdomen preparation, the suction electrode, extracellular amplifier and input probe and the Arduino control box. This particular orientation is for the linear stretch of the tail. For the tail curl, the tail is rotated 180° with respect to the Arduino puller box. Any extracellular amplifier that can provide differential recording between the two suction electrode wires and accept a bath ground input would suffice for recording (see Land et al., 2001).

APPENDIX VII
SCHEMATIC DIAGRAM SHOWING CIRCUIT CONNECTIONS FOR ARDUINO CONTROL BOX

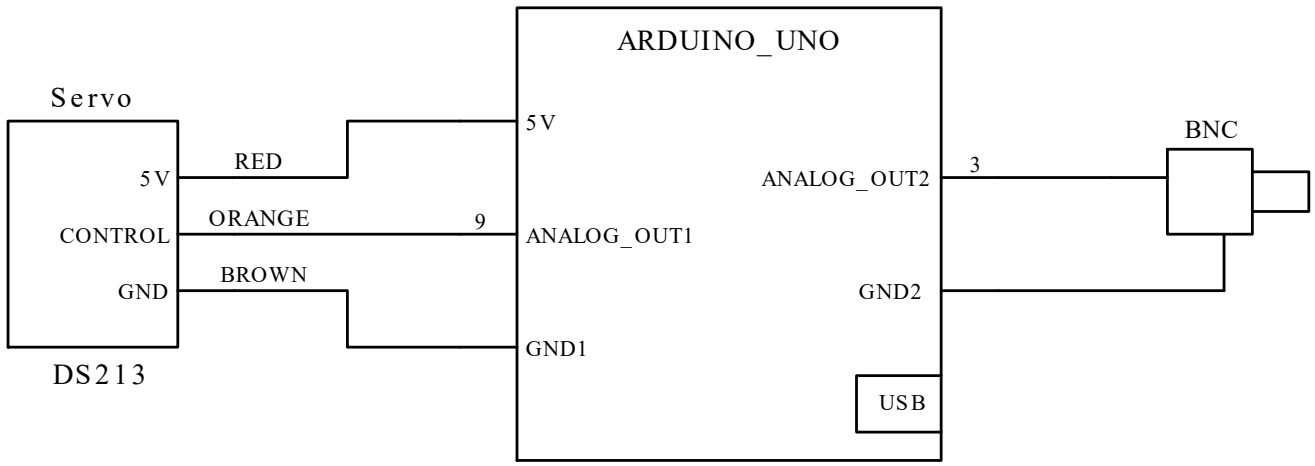

Figure A3. Circuit diagram to show input and output connections and device wiring of the Arduino control box. The small numbers (3, 9) indicate the socket numbers on the Arduino board used to plug in the respective connection wires.

APPENDIX VIII
TECHNICAL SPECIFICATIONS FOR THE DAVIGA DS213 ROTARY ACTUATOR

Servo Type	Digital
Gear Type	Metal
Stall Torque	2.5Kg.cm@4.8V, 3Kg.cm@6.0V
Speed	0.08sec/60º@4.8V, 0.07sec/60º@6.0V
Dimensions	23.1 x 12 x 24.5 mm
Weight	16 g
Operating Voltage	4.5V to 6V
Potentiometer	Direct Drive
Ball Bearings	2
Device Shell	Aluminum Alloy

The rotary actuator specified above was chosen after testing several other models to determine which rotary actuator could produce the torque and speed adequate to activate both the phasic and tonic MROs, while also remaining relatively still at a particular command voltage. We found that the best servos by these criteria were in the $25-30 price range. The MRO pull speed is measured from the readout of the position sensor build into the actuator.

APPENDIX IX
SOURCE CODE FOR ARDUINO-CONTROLLED STIMULATOR

A downloadable .ino file is accessible at https://github.com/neu350/MRO.

```
#include <Servo.h>

Servo myservo;  // create servo object to control a servo

int pos=0;           // target position for each function call (in mm displacement)
char ch;             // initialize serial byte variable
int outPin=3;
int anlgOut=0;
int target=0;        // target position in microseconds
int current=2000;    // incremental position in microseconds
int increment = 0;   // step size according to speed


void setup()
{
  Serial.begin(9600); // initialize serial connection, baud rate 9600
  myservo.attach(9);  // attaches the servo on pin 9 to the servo object
  myservo.writeMicroseconds(2000);
  Serial.println("Servo Control Clockwise Pull V1.3"); // display in serial monitor
  Serial.println("Enter command: ");
}

void loop()
{

  if ( Serial.available()>0) {
    ch = Serial.read();


    switch(ch) {

      case '0'...'9':
        pos = pos*10+ch-'0';
        pos = constrain(pos,0,179);
        target=map(pos,0,30,2000,1000);
// this map statement changes if you want a ccw pull instead of clockwise;
// switch 2000 and 1000 to reverse
        break;

      case 'f':
```

```
        current = target;
        myservo.writeMicroseconds(current);
        anlgOut=map(current,1000,2000,1,254);
        analogWrite(outPin,anlgOut);
        pos=0;
        break;

      case 'r':
        pos=0;
        for (current; current<=2000; current-=10) {
//reverse to zero also changes: >=1000 instead of <=2000.
        myservo.writeMicroseconds(current);
        anlgOut=map(current,1000,2000,1,254);
        analogWrite(outPin,anlgOut);
        delay(10);
        }
        break;

      case 'a':
        increment = 2;

        if (current < target) {
          extend(current, target, increment);
        }
        else if (current > target) {
          retract(current, target, increment);
        }

        current = target;
        pos = 0;
        break;

      case 'b':
        increment = 4;

        if (current < target) {
          extend(current, target, increment);
        }
        else if (current > target) {
          retract(current, target, increment);
        }

        current = target;
        pos = 0;
        break;

      case 'c':
        increment = 6;

        if (current < target) {
          extend(current, target, increment);
        }
        else if (current > target) {
          retract(current, target, increment);
        }

        current = target;
        pos = 0;
        break;

      case 'd':
         increment = 8;

        if (current < target) {
          extend(current, target, increment);
        }
        else if (current > target) {
          retract(current, target, increment);
        }

        current = target;
        pos = 0;
        break;

      case 'e':
```

```
        increment = 10;

        if (current < target) {
          extend(current, target, increment);
        }
        else if (current > target) {
          retract(current, target, increment);
        }

        current = target;
        pos = 0;
        break;
    }
  }
  else
  {
  anlgOut=map(current,1000,2000,1,254);
  analogWrite(outPin,anlgOut);
  }
}

void extend(int current, int target, int increment)
{
  for(current; current <= target; current+=increment) {
    myservo.writeMicroseconds(current);
    anlgOut=map(current,1000,2000,1,254);
    analogWrite(outPin,anlgOut);
    delay(10);
  }
}

void retract(int current, int target, int decrement)
{
  for(current; current >= target; current-=decrement) {
    myservo.writeMicroseconds(current);
    anlgOut=map(current,1000,2000,1,254);
    analogWrite(outPin,anlgOut);
    delay(10);
  }
}
```

APPENDIX X
PYTHON 3.X SOURCE CODE FOR GRAPHICAL USER INTERFACE

A downloadable .py file is accessible at https://github.com/neu350/MRO.

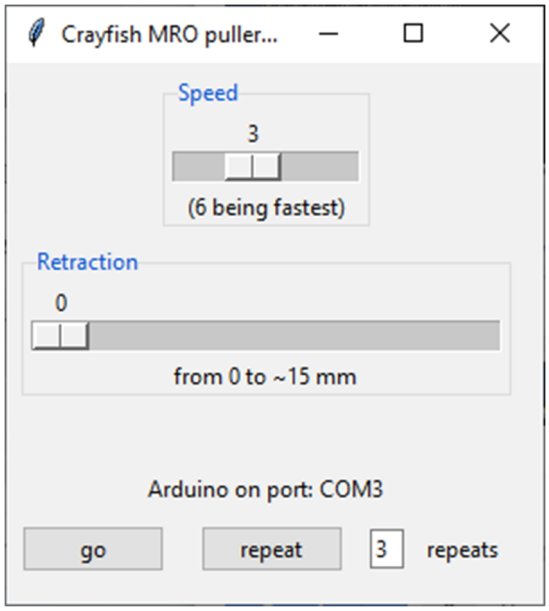

Figure J1. Screenshot of python GUI for Arduino puller.

```
from tkinter import *
from tkinter import font
from tkinter import ttk

import serial
import serial.tools.list_ports
import time

arduinoPort = "/dev/cu.usbmodem1411"

# the port should be detected automatically.  what you should use as default when it is not
# auto-detected will vary by OS.

all_ports = list(serial.tools.list_ports.comports()) # list of a 3-tuple for each port
ports = [(port, desc) for port, desc, hwid in all_ports if "Arduino" in desc]
if len(ports) > 0:
    arduinoPort, arduinoDesc = ports[0]
    print("Detected port: %s (%s)" % (arduinoPort, arduinoDesc))
else:
    print("Could not auto-detect port. Using %s as default." % arduinoPort)
    print("Ports:")
    print(all_ports)

ser = serial.Serial(arduinoPort, 9600)

def go(*args):
    try:
        speeds = ['null','a','b','c','d','e','f']
        spdi = int(speed.get())
        spd = speeds[spdi]
        pos = coord.get()

        cmd = format("%d%s" % (pos,spd))

        command.set(cmd)
        iibyte=bytearray(cmd,'ascii')
        ser.write(iibyte)
        #        print(ii)
        print(iibyte)
    except ValueError:
```

```
        pass

def zero(*args):
    try:
        speeds = ['null','a','b','c','d','e','f']
        spdi = int(speed.get())
        spd = speeds[spdi]
        pos = 0

        cmd = format("%d%s" % (pos,spd))

        command.set(cmd)
        iibyte=bytearray(cmd,'ascii')
        ser.write(iibyte)
    except ValueError:
        pass

def repeat(*args):
    try:
        repeati=int(repeats.get());
        zero()
        time.sleep(3)

        for i in range(0,repeati):
            print(i)
            go()
            time.sleep(3)
            zero()
            time.sleep(3)
    except ValueError:
        pass

root = Tk()
root.title("Crayfish MRO puller interface")

command = StringVar()

mainframe = ttk.Frame(root, padding="3 3 12 12")
mainframe.grid(column=0, row=0, sticky=(N, W, E, S))
mainframe.columnconfigure(0, weight=1)
mainframe.rowconfigure(0, weight=1)

headFont = font.Font(family='Helvetica', size=16, weight='bold')
smallFont = font.Font(family='Helvetica', size=8)

porty = StringVar()
porty = "Arduino on port: %s" % arduinoPort
ttk.Label(mainframe, text=porty).grid(column=1, row=8, columnspan=4)

ttk.Label(mainframe, textvariable=command).grid(column=1, row=6, sticky=S, columnspan=4)

speed = DoubleVar()
speedframe = ttk.Labelframe(mainframe, text='Speed')
slider = Scale(speedframe, orient=HORIZONTAL, variable=speed, length=100, from_=1, to=6, \
      resolution=1).grid(column=1, row=2)
ttk.Label(speedframe, text="(6 being fastest)").grid(column=1, row=4, sticky=N)
speed.set(3)
speedframe.grid(column=1,row=1,columnspan=4)

# the Arduino will translate this coordinate to a position on a 90 degree arc of the servo's
# range. The actual retraction length this corresponds to will depend on the length of the arm
# mounted to the servo.

coord = DoubleVar()
coordframe = ttk.Labelframe(mainframe, text='Retraction')
slider = Scale(coordframe, orient=HORIZONTAL, variable=coord, length=250, from_=0, to=30, \
      resolution=1).grid(column=1, row=2)
ttk.Label(coordframe, text="from 0 to ~30 mm").grid(column=1, row=4, sticky=N)
coord.set(0)
coordframe.grid(column=1,row=2,columnspan=4)

ttk.Button(mainframe, text="go", command=go).grid(column=1, row=9, sticky=W)
ttk.Button(mainframe, text="repeat", command=repeat).grid(column=2, row=9, sticky=E)

repeats = DoubleVar()
```

```
repeatentry = ttk.Entry(mainframe, textvariable=repeats, width=2).grid(column=3, row=9, sticky=E)
repeats.set(3)
ttk.Label(mainframe, text="repeats").grid(column=4, row=9, sticky=W)

for child in mainframe.winfo_children(): child.grid_configure(padx=5, pady=5)

root.bind('<Return>', go)

root.mainloop()
```